

## CONCLUSION

We assessed the dynamics of the VSCC-ocular reflex in normal subjects and then compared its gain in normal subjects to that of patients with BPPV. Our findings indicate that BPPV caused by canalolithiasis does not change the VOR gain of the VSCC at all frequencies, and that the mass of free-floating otocorial debris associated with canalolithiasis is too small compared to that of the endolymph to change the canal dynamics.

## ACKNOWLEDGMENT

This study was supported by a Health Science Research Grant for Specific Disease of the Ministry for Health and Welfare, Japan and a Grant-in-Aid for Scientific Research from the Japan Society for the Promotion of Science.

## REFERENCES

- Morita M. Testing of vertical semicircular canal-stimulative postrotatory nystagmus. *Equilibrium Res* 1993; 52: 461–5.
- Morita M, Takeda N, Koizuka I, Kubo T. Vertical semicircular canal-stimulative post-rotatory nystagmus. *Equilibrium Res* 1996; 55: 380–6.
- Morita M, Imai T, Sekine K, Takeda N, Koizuka I, Uno A, et al. A new rotational test for vertical semicircular canal function. *Auris Nasus Larynx* 2003; 30: 233–7.
- Decher H. Experimental labyrinthine tests on isolated individual semicircular canals as fitness test for astronauts. *Aerosp Med* 1969; 40: 1203–8.
- Imai T, Takeda N, Morita M, Koizuka I, Kubo T, Miura K, et al. Rotation vector analysis of eye movement in three dimensions with an infrared CCD camera. *Acta Otolaryngol (Stockh)* 1999; 119: 24–8.
- Blanks RH, Curthoys IS, Markham CH. Planar relationships of the semicircular canals in man. *Acta Otolaryngol (Stockh)* 1975; 80: 185–96.
- Cremer PD, Halmagyi GM, Aw ST, Curthoys IS, McGarvie LA, Todd MJ, et al. Semicircular canal plane head impulses detect absent function of individual semicircular canals. *Brain* 1998; 121: 699–716.
- Kanayama R, Bronstein AM, Gresty MA, Brookes GB. Vertical and torsional VOR in posterior canal occlusion. *Acta Otolaryngol Suppl (Stockh)* 1995; 520: 362–5.
- Marquardt DW. An algorithm for least-squares estimation of non-linear parameters. *J Soc Ind Appl Math* 1963; 11: 431–41.
- Fetter M, Zee DS, Tweed D, Koenig E. Head position dependent adjustment of the three-dimensional human vestibuloocular reflex. *Acta Otolaryngol (Stockh)* 1994; 114: 473–8.
- Baloh RW, Horubia V, Konrad HR. Ewald's second law re-evaluated. *Arch Otolaryngol* 1977; 83: 475–9.
- Baloh RW, Hess K, Horubia V, Yee RD. Low and high frequency sinusoidal rotational testing in patients with peripheral vestibular lesions. *Acta Otolaryngol Suppl (Stockh)* 1984; 406: 189–93.
- Wall III C, Black FO. Intersubject variability in VOR responses to 0.005–1.0 Hz sinusoidal rotations. *Acta Otolaryngol Suppl (Stockh)* 1984; 406: 194–8.
- Paige GD. Nonlinearity and asymmetry in the human vestibular-ocular reflex. *Acta Otolaryngol (Stockh)* 1989; 108: 1–8.
- Tweed D, Sievering D, Misslich H, Fetter M, Zee D, Koenig E. Rotation kinematics of the human vestibular reflex. I. Gain matrices. *J Neurophysiol* 1994; 72: 2467–79.
- Iida M, Hitouji K, Takahashi M. Vertical semicircular canal function: a study in patients with benign paroxysmal positional vertigo. *Acta Otolaryngol Suppl* 2001; 545: 35–7.
- Epley JM. New dimensions of benign paroxysmal positional vertigo. *Otolaryngol Head Neck Surg* 1980; 88: 599–605.
- Parnes LS, McClure JA. Free floating endolymph particles: a new operative finding during posterior semicircular canal occlusion. *Laryngoscope* 1992; 102: 988–92.
- Sekine K, Iami T, Nakamae K, Miura K, Fujioka H, Takeda N. Dynamics of vestibulo-ocular reflex in patients with horizontal semicircular canal variant of benign paroxysmal positional vertigo. *Acta Otolaryngol* 2003, in press.

*Submitted January 26, 2004; accepted February 26, 2004*

Address for correspondence:  
Kazunori Sekine, MD  
Department of Otolaryngology  
University of Tokushima School of Medicine  
3-18-15 Kuramoto  
Tokushima 770-8503  
Japan  
Fax: +81 88 633 7170  
E-mail: seky@clin.med.tokushima-u.ac.jp

## Dynamics of the Vestibulo-ocular Reflex in Patients with the Horizontal Semicircular Canal Variant of Benign Paroxysmal Positional Vertigo

KAZUNORI SEKINE<sup>1</sup>, TAKAO IMAI<sup>2</sup>, KOJI NAKAMAE<sup>3</sup>, KATSUYOSHI MIURA<sup>3</sup>, HIROMU FUJIOKA<sup>3</sup> and NORIAKI TAKEDA<sup>1</sup>

From the <sup>1</sup>Department of Otolaryngology, University of Tokushima School of Medicine, Tokushima, Japan, <sup>2</sup>Department of Otolaryngology and Sensory Organ Surgery, Osaka University Graduate School of Medicine, Osaka, Japan and <sup>3</sup>Department of Information Systems Engineering, Osaka University Graduate School of Engineering, Osaka, Japan

Sekine K, Imai T, Nakamae K, Miura K, Fujioka H, Takeda N. Dynamics of the vestibulo-ocular reflex in patients with the horizontal semicircular canal variant of benign paroxysmal positional vertigo. *Acta Otolaryngol* 2004; 124: 587–594.

**Objective**—Two types of direction-changing positional nystagmus, the geotropic and apogeotropic variants, are observed in patients with the horizontal semicircular canal (HSCC) type of benign paroxysmal positional vertigo (H-BPPV). In this study, we assessed the dynamics of the vestibulo-ocular reflex (VOR) of the HSCC in patients with H-BPPV.

**Material and Methods**—Patients were rotated about the earth-vertical axis at frequencies of 0.1, 0.3, 0.5, 0.7 and 1.0 Hz with a maximum angular velocity of 50°/s. Eye movements were recorded on a video imaging system using an infrared charge-coupled device (CCD) camera, and our new technique for analyzing the rotation vector of eye movements in three dimensions was used.

**Results**—In the patients with geotropic positional nystagmus, there were no differences in VOR gain between rotation to the affected and unaffected sides at frequencies of 0.1–1.0 Hz. Although no differences in VOR gain at frequencies of 0.3–1.0 Hz were noticed in patients with apogeotropic positional nystagmus, the VOR gain at 0.1 Hz was significantly smaller on rotation to the affected compared to the unaffected side.

**Conclusion**—The results indicate that cupulolithiasis in the HSCC affected the dynamics of the HSCC-ocular reflex at 0.1 Hz, but not at higher frequencies, and that canalolithiasis in the HSCC does not change the VOR gain of the HSCC at any frequency. It is suggested that cupulolithiasis causes transient impairment of HSCC function by means of its mechanical restriction of movements of the cupula. *Key words:* apogeotropic positional nystagmus, benign paroxysmal positional vertigo, direction-changing nystagmus, geotropic positional nystagmus.

### INTRODUCTION

Benign paroxysmal positional vertigo (BPPV) is a common vestibular disorder characterized by brief episodes of vertigo triggered by changes in head position. Most instances of BPPV are caused by a lesion in the posterior semicircular canal. Recently, however, many authors (1–4) have reported another type of BPPV, in which the horizontal semicircular canal (HSCC) is affected. This variant of BPPV (H-BPPV) is elicited when rolling the head from side to side whilst lying in a supine position.

Two types of direction-changing positional nystagmus, the geotropic and apogeotropic variants, are observed in patients with H-BPPV. It has been hypothesized that geotropic positional nystagmus of H-BPPV is induced by canalolithiasis in the HSCC (1–4) and that the apogeotropic type of H-BPPV is triggered by cupulolithiasis of the HSCC (5, 6). Based on the canalolithiasis hypothesis, free-floating otoconial debris in the HSCC acts like a plunger, causing movement of the endolymph during changes in head position (7, 8). In contrast, the cupulolithiasis hypothesis asserts that the cupula becomes heavier by being attached to otoconial debris, and thus responds to changes in head position (9). Therefore, it is possible that canalolithiasis and cupulolithiasis change the

dynamics of the vestibular-ocular reflex (VOR) elicited by HSCC stimulation.

In this study, we assessed the dynamics of HSCC-induced VOR in patients with H-BPPV using our new technique for analyzing the rotation vector of eye movement in three dimensions (10). The VOR gain of patients with geotropic positional nystagmus was then compared with that of apogeotropic positional nystagmus.

### MATERIAL AND METHODS

#### Subjects

The study subjects comprised nine patients with H-BPPV. Of these, 5 (1 male, 4 females; age range 42–65 years; mean age 53.0±9.5 years) had apogeotropic and 4 (1 male, 3 females; age range 54–70 years; mean age 63.0±6.1 years) geotropic nystagmus. H-BPPV was diagnosed by means of the following criteria:

1. Absence of an identifiable central nervous system disorder able to explain the positional vertigo following neurological and neuroradiological studies.
2. Absence of spontaneous nystagmus.
3. A history of brief episodes of positional vertigo.

4. Observation of a direction-changing positional nystagmus with a main horizontal component triggered by lying in the supine position and head rotations.
5. The geotropic variant was indicated by positional vertigo with a short latency of  $\leq 60$  s.
6. The apogeotropic variant was indicated by an intense nystagmus that reached its maximum intensity immediately after a change of head position and lasted for  $> 1$  min.

In all patients, the affected ear was determined as follows (4–6). In the case of geotropic positional nystagmus, the intensity of positional nystagmus was a maximum when the head was rotated to the affected side while supine. In the apogeotropic variant, the intensity of positional nystagmus was a minimum when the head was rotated to the affected side while supine.

The study was performed in accordance with the guidelines approved by the Committee for Medical Ethics of the University of Tokushima School of Medicine and informed consent was obtained from each patient prior to the rotation test.

#### *Experimental protocols*

Patients were seated on a computer-controlled rotating chair with their head tilted  $30^\circ$  forward and rotated around the earth-vertical axis sinusoidally with eyes open in complete darkness at frequencies of 0.1, 0.3, 0.5, 0.7 and 1.0 Hz with a maximum angular velocity of  $50^\circ/\text{s}$ . To maintain alertness during rotation, subjects were asked to perform mental arithmetic during the whole procedure. The interval between rotational tests performed using different rotational frequencies was  $> 5$  min.

#### *Recording system and data analysis*

Eye movements were recorded as digital images ( $720 \times 480$  dots) using an infrared charge-coupled device camera trained on the left eye. The sampling rate of digital images was 30 Hz. The center of eye rotation on the image plane was determined as the point, and the radius of the eyeballs calculated. The center of the pupil and an iris freckle on each digital image were also determined as the point on the image plane. The point of the center of the pupil and an iris freckle on the image plane were identified and reconstructed in the 3D head coordinates of the center of the pupil and an iris freckle, determined by the point of the center of eye rotation on the image plane and the radius of the eyeball. The rotation vectors of the eye position in three dimensions were calculated from the head coordinates of the center of the pupil and an iris freckle. In order to calculate the exact VOR

gain, which is the ratio of the compensatory eye velocity around the rotation axis to the head velocity, the rotation vector but not the Fick coordinates of the eye movement must be analyzed. The eye velocity around the rotation axis was derived from the rotation vectors of the eye position. The method used to analyze the eye rotation vectors has been described elsewhere (10). We calculated eye velocities around the rotation axis as the magnitude of the rotation vector that represents the velocity. These values of eye velocities were positive when unrelated to the direction of eye rotation. To express eye velocities around the rotation axis as right-handed, the mark of the velocities around the rotation was synchronized to that of the Z component, the largest of all the components. Fast eye movements were removed to give cumulative slow-phase eye velocities. After synchronizing the mark and removing fast eye movements, eye velocities were approximated by the best-fitting sine curve for each rightward and leftward eye movement using the least-squares method (11). The frontal gaze eye position was chosen as the reference point. Head coordinates (X, Y, Z) were defined using the right-handed rule, so that the X axis was parallel to the naso-occipital axis (positive forward), the Y axis parallel to the inter-aural axis (positive left) and the Z axis normal to the XY plane (positive upwards).

We determined the maximum slow-phase eye velocity (MSPV) on rotation to the affected and unaffected sides about the rotation axis from the best-fitting sine curve, and the VOR gain was calculated as the ratio of the MSPV to the maximum head angular velocity ( $50^\circ/\text{s}$ ). The directional preponderance (DP) of per-rotatory nystagmus was calculated as follows:

$$\text{DP (\%)} = \left[ \frac{(\text{MSPV on rotation to the unaffected side}) - (\text{MSPV on rotation to the affected side})}{(\text{MSPV on rotation to the unaffected side}) + (\text{MSPV on rotation to the affected side})} \right] \times 100.$$

#### *Statistical analysis*

Changes in VOR gain were tested by means of repeat-measures ANOVA. Further comparisons at each frequency were analyzed using the Bonferroni–Dunn test and  $p < 0.05$  was considered significant.

## RESULTS

Fig. 1 shows the 3D angular eye positions and angular eye velocities of per-rotatory nystagmus when a patient with geotropic positional nystagmus was

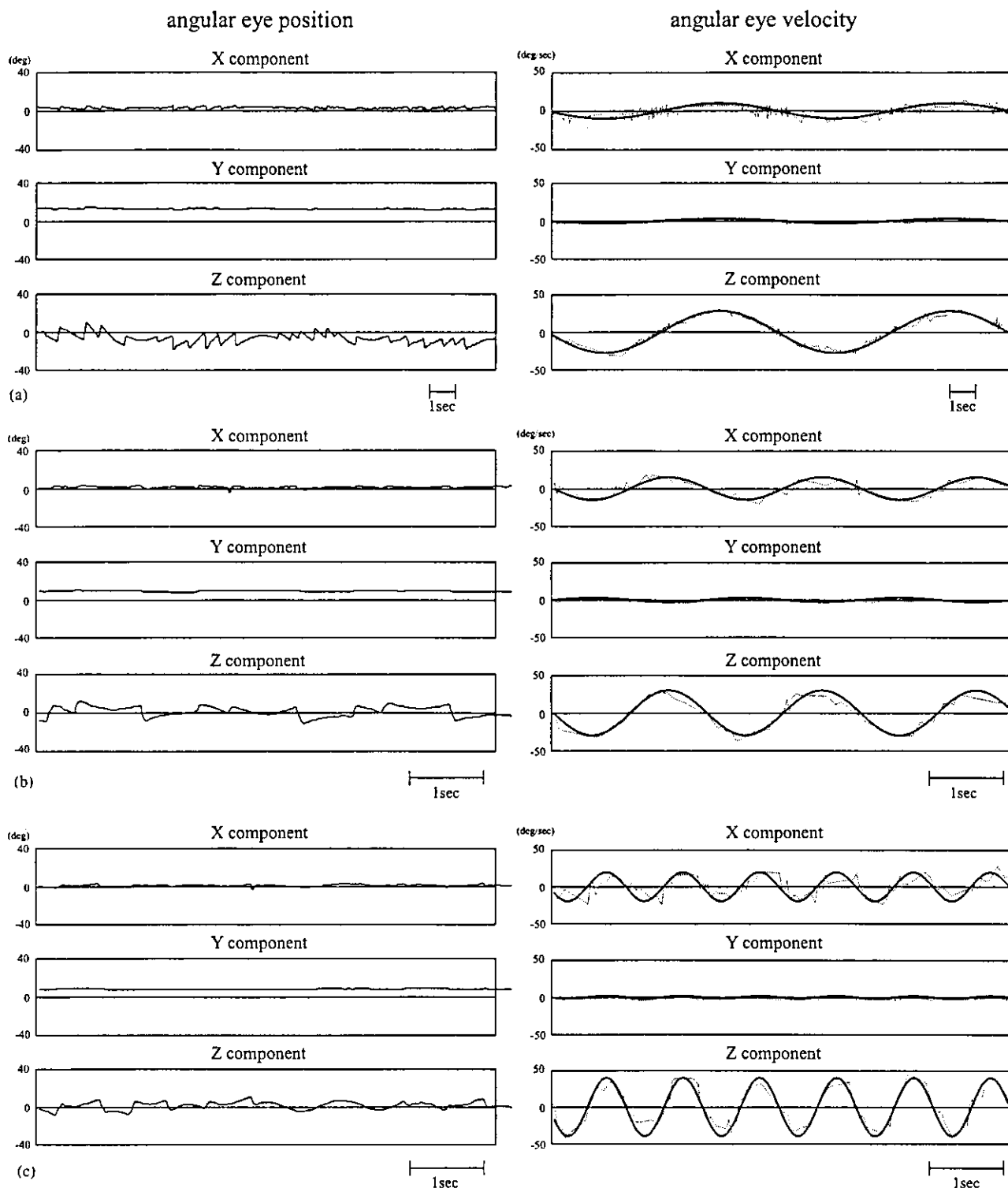


Fig. 1. X, Y and Z components of angular eye positions and angular eye velocities of per-rotatory nystagmus in a patient with geotropic positional nystagmus: (a) 0.1 Hz; (b) 0.5 Hz; (c) 1.0 Hz.

rotated at frequencies of 0.1, 0.5 and 1.0 Hz. Fig. 2 shows the same eye positions and velocities when a patient with apogeotropic positional nystagmus was rotated at the same frequencies. The angular eye

velocity mainly consisted of a Z component, with a small X component, in both patients. The eye velocity vectors of per-rotatory nystagmus were plotted on the XY, XZ and YZ planes in patients with geotropic and

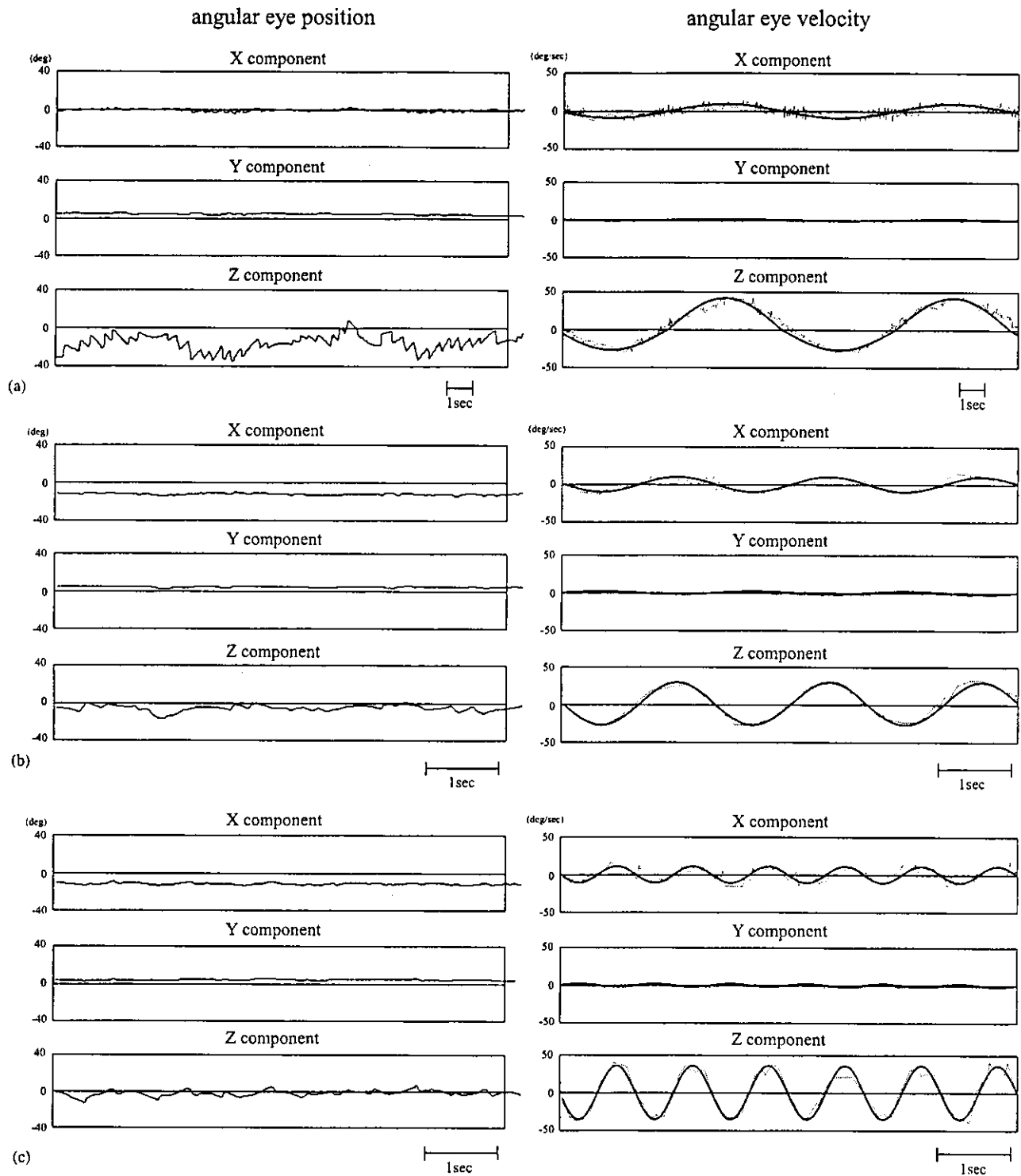


Fig. 2. X, Y and Z components of angular eye positions and angular eye velocities of per-rotatory nystagmus in a patient with apogeotropic positional nystagmus: (a) 0.1 Hz; (b) 0.5 Hz; (c) 1.0 Hz.

apogeotropic positional nystagmus (Fig. 3). The axis of the eye velocity vectors of per-rotatory nystagmus was tilted almost 30° backward and approximately aligned with the axis of head rotation, but not with the

yaw axis. Fig. 4 shows the angular eye velocity of per-rotatory nystagmus around the rotation axis in patients with geotropic and apogeotropic positional nystagmus. In order to calculate the VOR gain, we

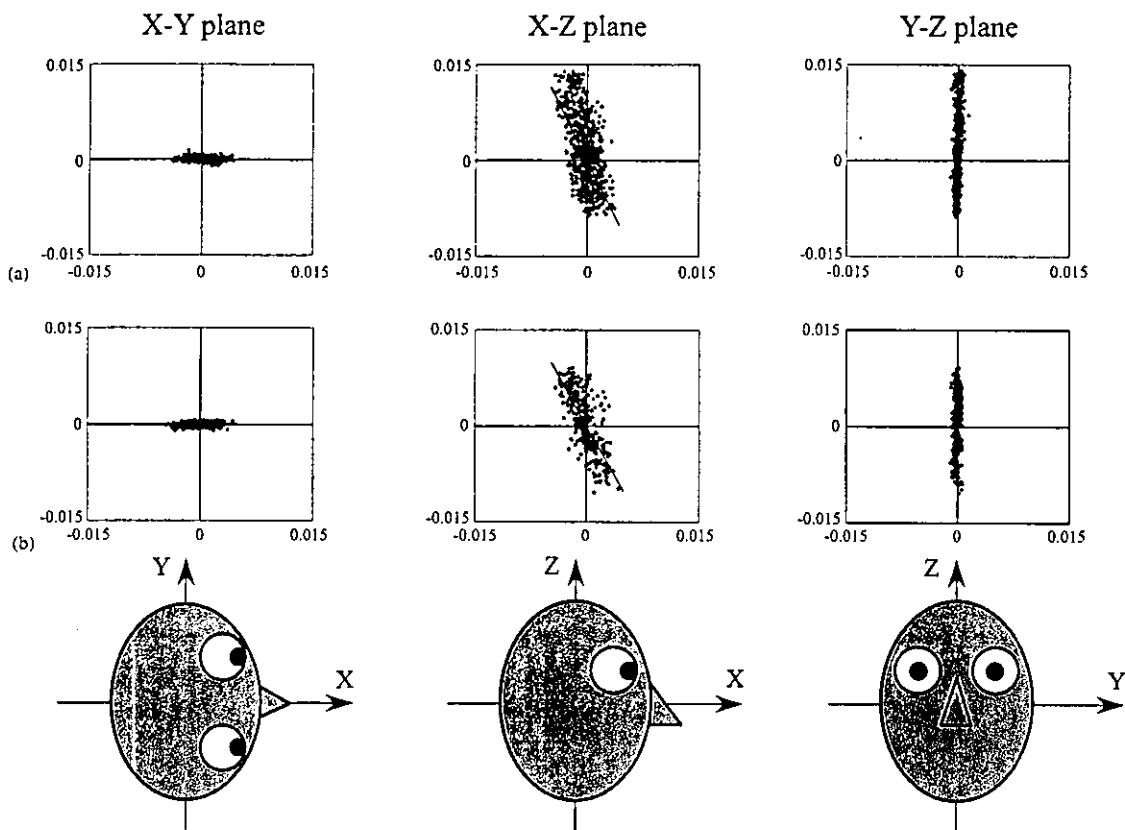


Fig. 3. Eye velocity vectors of per-rotatory nystagmus in the XY, XZ and YZ planes in patients with (a) apogeotropic and (b) geotropic positional nystagmus.

used the slow-phase angular eye velocity of per-rotatory nystagmus around the rotation axis.

The mean VOR gains in patients with geotropic positional nystagmus were 0.62, 0.71, 0.72, 0.84 and 0.85 at 0.1, 0.3, 0.5, 0.7 and 1.0 Hz, respectively on rotation to the affected side and 0.62, 0.68, 0.69, 0.81 and 0.83 at 0.1, 0.3, 0.5, 0.7 and 1.0 Hz, respectively on rotation to the unaffected side (Fig. 5a). No significant difference was noticed in the VOR gain between the affected and unaffected sides at any frequency.

The mean VOR gains in patients with apogeotropic positional nystagmus were 0.44, 0.51, 0.59, 0.62 and 0.81 at 0.1, 0.3, 0.5, 0.7 and 1.0 Hz, respectively on rotation to the affected side and 0.74, 0.60, 0.62, 0.64 and 0.81 at 0.1, 0.3, 0.5, 0.7 and 1.0 Hz, respectively on rotation to the unaffected side (Fig. 5b). Here also the VOR gain at frequencies of 0.3–1.0 Hz showed no significant differences on rotation to the affected or unaffected sides. However, at 0.1 Hz the VOR gain on rotation to the affected side was significantly smaller on rotation to the unaffected side ( $p < 0.05$ ).

The DP of per-rotatory nystagmus in patients with geotropic and apogeotropic positional nystagmus is shown in Fig. 6. There was no asymmetry in patients

with geotropic positional nystagmus; however, a DP of per-rotatory nystagmus to the unaffected side was evident at 0.1 Hz in patients with the apogeotropic variant and gradually decreased with increasing frequency.

Fig. 7 shows changes in the DP of per-rotatory nystagmus in a patient whose positional nystagmus was transformed from apogeotropic to geotropic after therapeutic head shaking. When the patient showed apogeotropic positional nystagmus, the DP was evident to the affected side at 0.1 Hz, but this disappeared after conversion to the geotropic variant.

## DISCUSSION

Based on the canalolithiasis hypothesis of H-BPPV (1–4), when the patient lies in a supine position and turns his/her head toward the affected side, free-floating debris causes an ampullopetal endolymph flow in the homolateral HSCC. In contrast, when the patient turns his/her head toward the unaffected side, an ampulofugal endolymph flow is generated in the affected HSCC. According to Ewald's second law (12), canalolithiasis in the HSCC induces geotropic positional nystagmus, the intensity of which is maximal

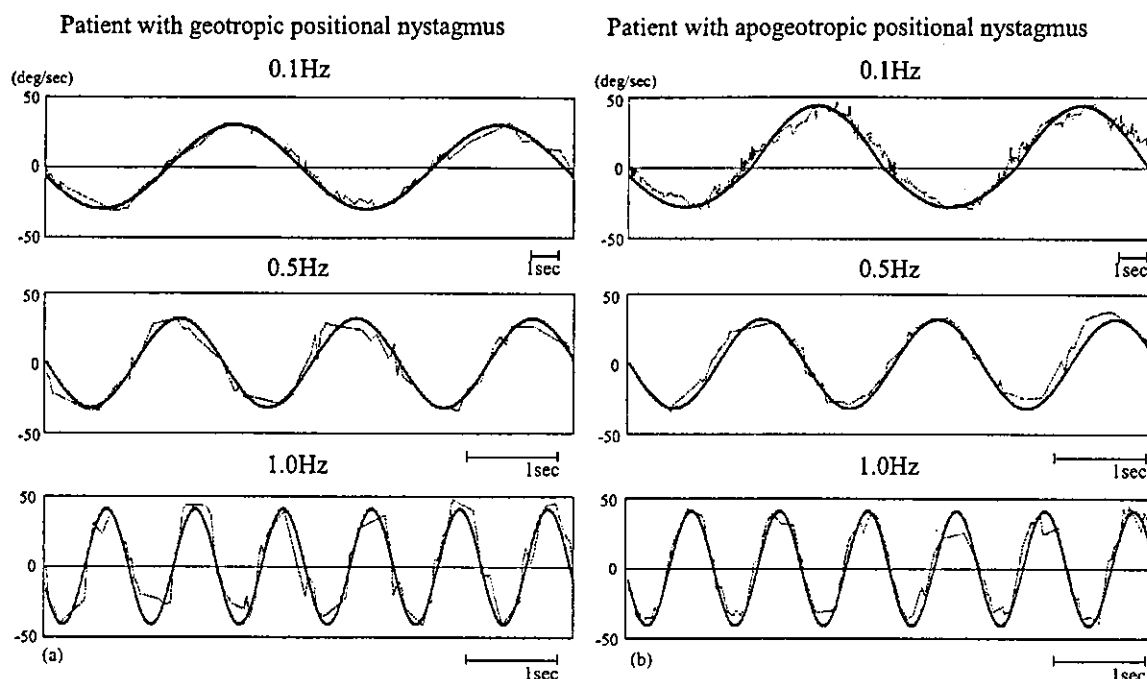


Fig. 4. Angular eye velocities of per-rotatory nystagmus about the rotation axis in patients with (a) geotropic and (b) apogeotropic positional nystagmus.

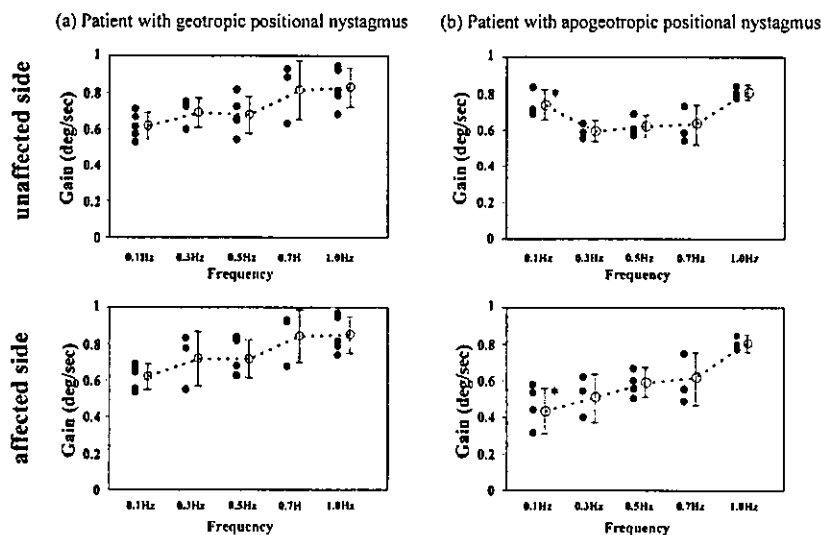


Fig. 5. VOR gain on rotation to the affected and unaffected sides in patients with (a) geotropic and (b) apogeotropic positional nystagmus. \* $p < 0.05$ .

when the head is turned to the affected side. Based on the cupulolithiasis hypothesis of H-BPPV (5, 6), when the patient turns his/her head toward the affected side, a heavy cupula causes an ampullofugal endolymph flow in that HSCC. In contrast, when the patient turns his/her head toward the unaffected side, an ampullopetal endolymph flow is triggered in the affected HSCC. According to Ewald's second law (12), cupulolithiasis in the HSCC induces apogeotropic posi-

tional nystagmus, the intensity of which is maximal when the head is turned to the unaffected side (4).

In the present study, we assessed the dynamics of the VOR in the HSCC of patients with H-BPPV, because it would be expected that canalolithiasis or cupulolithiasis would alter canal dynamics. In patients with apogeotropic positional nystagmus, the VOR gain at 0.1 Hz was significantly smaller on rotation to the affected compared to the unaffected side (Fig.

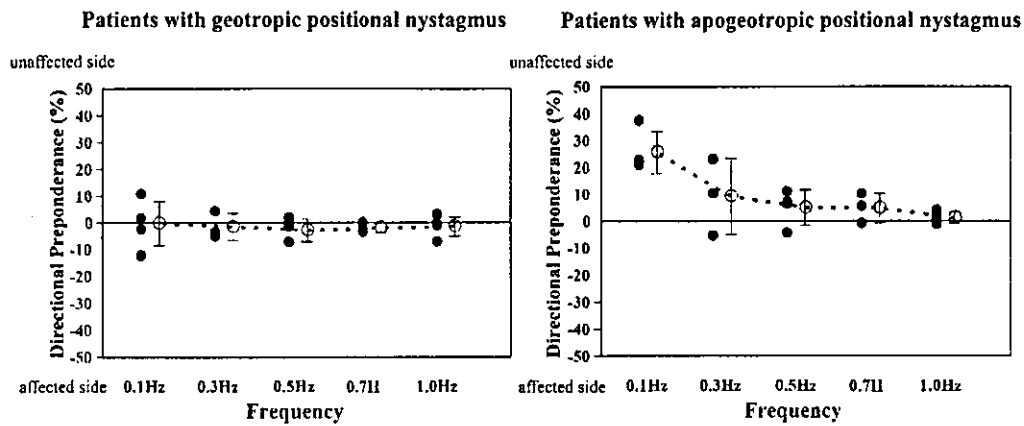


Fig. 6. DP of per-rotatory nystagmus in patients with geotropic and apogeotropic nystagmus.

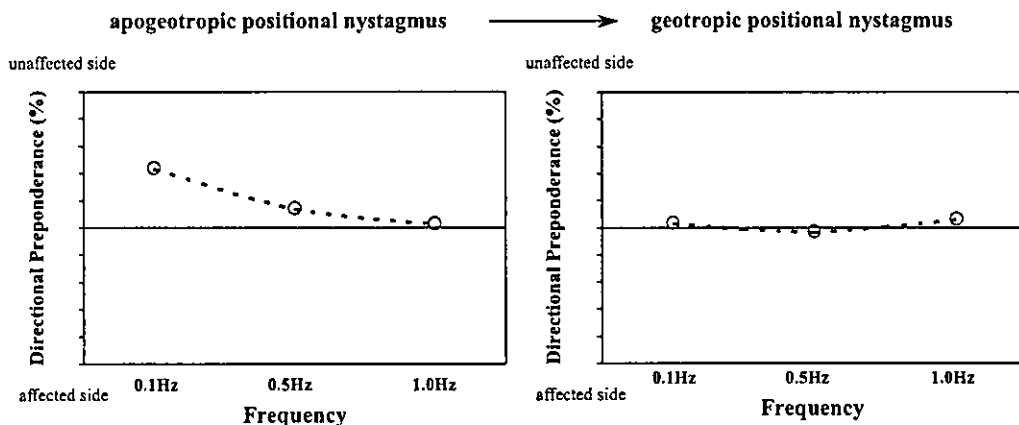


Fig. 7. Changes in DP of per-rotatory nystagmus in a patient whose positional nystagmus was transformed from apogeotropic to geotropic.

5b). The reduced VOR gain on rotation to the affected side suggests a decreased sensitivity of the HSCC due to cupulolithiasis. In fact, Baloh et al. (12) reported that VOR responses were decreased for head rotation toward the lesioned side in patients with unilateral labyrinthectomy. It was also reported that VOR gain on active head rotation toward the affected side was reduced in patients with unilateral vestibular lesions (13). Because cupulolithiasis is assumed to be caused by otoconial debris attached to the cupula, it is suggested that cupulolithiasis restricts the movements of the cupula, resulting in loss of HSCC sensitivity.

The reduced VOR gain on rotation to the affected side (Fig. 5b) and the evidence of DP of per-rotatory nystagmus (Fig. 6) at 0.1 Hz, but not at higher frequencies, are not consistent with previous findings. Indeed, Baloh et al. (14) reported that, in patients with unilateral vestibular lesions, asymmetries in VOR gain were approximately the same at frequencies of 0.01–2.0 Hz. This finding was corroborated by the observa-

tion that the VOR gain on active head rotation to the affected side was almost half of that to the unaffected side at frequencies of 0.33, 0.67 and 1.0 Hz in patients with unilateral vestibular lesions (13). The difference between the present and previous findings can be explained by a transient functional, but not permanent, loss of sensitivity of the HSCC induced by cupulolithiasis. Because cupulolithiasis is assumed to be caused by otoconial debris attached to the cupula, it is suggested that mechanical restriction of the movement of the cupula due to cupulolithiasis at 0.1 Hz could be overcome by increased acceleration of endolymph at higher frequencies. In contrast, in patients with geotropic positional nystagmus, the VOR gain on rotation to the affected side was almost the same as that on rotation to the unaffected side (Fig. 5a), and DP of per-rotatory nystagmus was not evident at any of the frequencies of head rotation (Fig. 6). These results are in line with those reported by McClure (15), who found a reduced phase shift, but



no obvious change in VOR gain, during sinusoidal rotations of H-BPPV patients with geotropic positional nystagmus. This suggestion is based on the fact that the mass of free-floating otoconial debris associated with canalolithiasis is too small compared to the mass of the endolymph to alter the canal dynamics.

The DP of per-rotatory nystagmus changed in the patient whose positional nystagmus was transformed from apogeotropic to geotropic after therapeutic head shaking (16). Indeed, the DP of per-rotatory nystagmus at 0.1 Hz disappeared (Fig. 7), indicating that pathological transition from cupulolithiasis to canalolithiasis may lead to changes in the dynamics of HSCC-induced VOR.

## CONCLUSIONS

In this study, we assessed the dynamics of the VOR of the HSCC in patients with H-BPPV and compared the VOR gains of patients with geotropic and apogeotropic positional nystagmus. Our findings indicate that cupulolithiasis in the HSCC affects the dynamics of the HSCC-ocular reflex at 0.1 Hz, but not at higher frequencies, and that canalolithiasis in the HSCC does not change the VOR gain of the HSCC at any frequency. It is suggested that cupulolithiasis causes a transient impairment of HSCC function by means of mechanical restriction of movements of the cupula.

## ACKNOWLEDGEMENTS

This study was supported by a Health Science Research Grant for Specific Disease from the Ministry for Health and Welfare, Japan and a Grant-in-Aid for Scientific Research from the Japan Society for the Promotion of Science.

## REFERENCES

- McClure JA. Horizontal canal BPV. *J Otolaryngol* 1985; 14: 30-5.
- Pagnini P, Nuti D, Vannuchi P. Benign paroxysmal vertigo in the horizontal canal. *ORL J Otorhinolaryngol Relat Spec* 1989; 51: 161-70.
- Baloh RW, Jacobson K, Horubia V. Horizontal semi-circular canal variant of benign positional vertigo. *Neurology* 1993; 43: 2542-9.
- Augusto PC, Giovanni V, Bruno F, Stefano B. The treatment of horizontal canal positional vertigo: our experience in 66 cases. *Laryngoscope* 2002; 112: 172-8.
- Baloh RW, Yue Q, Jacobson K, Horubia V. Persistent direction-changing positional nystagmus: another variant of benign positional nystagmus? *Neurology* 1995; 45: 1297-301.
- Casani A, Vannucci G, Fattori B, Ghilardi PL. Positional vertigo and ageotropic bi-directional nystagmus. *Laryngoscope* 1997; 107: 807-13.
- Epley JM. New dimensions of benign paroxysmal positional vertigo. *Otolaryngol Head Neck Surg* 1980; 88: 599-605.
- Parnes LS, McClure JA. Free floating endolymph particles: a new operative finding during posterior semicircular canal occlusion. *Laryngoscope* 1992; 102: 988-92.
- Schuknecht HF. Cupulolithiasis. *Arch Otolaryngol* 1969; 90: 765-78.
- Imai T, Takeda N, Morita M, et al. Rotation vector analysis of eye movement in three dimensions with an infrared CCD camera. *Acta Otolaryngol (Stockh)* 1999; 119: 24-8.
- Marquardt DW. An algorithm for least-squares estimation of non-linear parameters. *Journal of the Society for Industrial and Applied Mathematics* 1963; 11: 431-41.
- Baloh RW, Horubia V, Konrad HR. Ewald's second law re-evaluated. *Arch Otolaryngol* 1977; 83: 475-9.
- Nogami K, Uemura T, Iwamoto M. VOR gain and phase in active head rotation tests of normal subjects and patients with peripheral labyrinthine lesions. *Acta Otolaryngol (Stockh)* 1989; 107: 333-7.
- Baloh RW, Hess K, Horubia V, Yee RD. Low and high sinusoidal rotational testing in patients with peripheral vestibular lesions. *Acta Otolaryngol Suppl (Stockh)* 1984; 406: 189-93.
- McClure JA. Functional basis for horizontal canal BPV. In: Barber HO, Sharpe JA, eds. *Vestibular disorders*. London: Year Book Medical Publishers; 1988. p. 233-8.
- Steddin S, Ing D, Brandt T. Horizontal canal benign paroxysmal positional vertigo (h-BPPV): transition of canalolithiasis to cupulolithiasis. *Ann Neurol* 1996; 40: 918-22.

Submitted February 24, 2003; accepted May 22, 2003

Address for correspondence:  
Kazunori Sekine, MD  
Department of Otolaryngology  
University of Tokushima School of Medicine  
3-18-15 Kuramoto  
Tokushima 770-8503  
Japan  
Fax: +81 88 633 7170  
E-mail: seky@clin.med.tokushima-u.ac.jp

# Three-Dimensional Eye Rotation Axis Analysis of Benign Paroxysmal Positioning Nystagmus

Takao Imai<sup>a</sup> Noriaki Takeda<sup>b</sup> Atsuhiko Uno<sup>a</sup> Masahiro Morita<sup>a</sup>  
Izumi Koizuka<sup>c</sup> Takeshi Kubo<sup>a</sup>

<sup>a</sup>Department of Otolaryngology and Sensory Organ Surgery, Osaka University Graduate School of Medicine, Osaka; <sup>b</sup>Department of Otolaryngology, University of Tokushima School of Medicine, Tokushima, and <sup>c</sup>Department of Otolaryngology, Saint Marianna Medical School, Kanagawa, Japan

## Key Words

Benign paroxysmal positioning nystagmus · Canalolithiasis · Eye rotation axis · Infrared CCD camera · Three-dimensional eye rotation axis

## Abstract

We have developed a new technique for analyzing the rotation vector of eye movement with an infrared CCD camera [Imai et al.: *Acta Otolaryngol* 1999;119:24-28]. We used this technique to analyze the eye rotation axis of benign paroxysmal positioning nystagmus (BPPN) that was induced by the Dix-Hallpike maneuver in 14 patients with benign paroxysmal positioning vertigo (BPPV). Eye rotation axes of BPPN in 8 patients were closely perpendicular to the posterior canal of the undermost ear in the provocative head position. Under the hypothesis that BPPN is due to a mechanical stimulation of the posterior canal by canalolithiasis, this finding suggested that the posterior canal of the undermost ear is the lesion. On the other hand, eye rotation axes of BPPN in the other 6 patients were closely aligned with the naso-occipital axis. It is suggested that canalolithiasis induces endolymphatic flow in both posterior and anterior canals via the common crus and the summation of the

eye movements induced by stimulation of both the posterior and anterior canals rotates the eye along the naso-occipital axis.

Copyright © 2002 S. Karger AG, Basel

## Introduction

Benign paroxysmal positioning vertigo (BPPV) is the most common type of vertigo due to peripheral vestibular lesion. Robert Bárány initially described this clinical entity in 1921 [1]. Concomitant benign paroxysmal positioning nystagmus (BPPN) is characteristic of this type of vertigo, but its mechanism is not fully understood.

According to the canalolithiasis hypothesis [2-4], movement of the head back and to the side in the plane of posterior semicircular canal causes the otocania to move in an ampullofugal direction, producing ampullofugal displacement of the cupula due to the plunger effect of the otocania moving within the narrow canal. In electrophysiological study, Suzuki and Cohen [5, 6] demonstrated that electrical stimulation of single semicircular canal afferents in animals induced eye movements that lie in the plane of the canal. So by analyzing the eye rotation axis in BPPN, we can define what canal is the origin of BPPN.

KARGER

Fax +41 61 306 12 34  
E-Mail karger@karger.ch  
www.karger.com

© 2002 S. Karger AG, Basel  
0301-1569/02/0646-0417\$18.50/0

Accessible online at:  
www.karger.com/orl

Takao Imai, MD, PhD  
Department of Otolaryngology, Kansai-Rosai Hospital  
3-1-69 Inabasou, Amagasaki-shi, Hyogo 660-8511 (Japan)  
Tel. +81 6 6416 1221, Fax +81 6 6419 1870  
E-Mail imaitakao@hotmail.com

We have developed a new technique for analyzing the eye movement's rotation vector in three dimensions with an infrared CCD camera [7]. Using this technique, the present study analyzed the eye rotation axis and eye rotation velocity around the axis of BPPN induced by the Dix-Hallpike maneuver [8]. The purpose of this study was thus to define what canal was the origin of BPPN by analyzing its eye rotation axis.

## Subjects and Methods

Fourteen patients aged from 36 to 72 years (averaged age 56 years) were studied. There were 8 women and 6 men. Patients met the following criteria: (1) a history of brief episodes of positional vertigo, and (2) a characteristic torsional paroxysmal positional nystagmus. We defined the lower ear in positional vertigo as the affected ear. These patients had no other evidence of neurologic or otologic diseases. The right ear was affected in 9 patients; the left, in 5. The positioning nystagmus was induced by the Dix-Hallpike maneuver [8]: all the subjects were moved rapidly from the upright position to head-hanging position and nystagmus was recorded on videotape with an infrared CCD camera.

In this paper, when we described the eye movements in 3D, we used rotation vectors, which characterize the 3D eye position by a single rotation. Rotation vector is a vector with the direction of the vector given by the axis of the rotation, and its length proportional to the size of the rotation. An eye position can be reached by rotation of the eye from the reference position about a single axis. This eye position is represented by a vector along the single axis, which is a length proportional to the angle of the rotation. The reference position was defined as the position the eye assumes when the subject was looking straight ahead, while the head was kept upright. Straight ahead was defined as looking at a target which was exactly horizontally in front of the eye [9]. The analysis method of eye rotation vectors has already been described [7]. We converted the videotape images into digital images (640·480 dot), and from the digital images we reconstructed the space coordinates of the center of pupil and an iris freckle. These coordinates (X, Y, Z) were defined such that X axis was parallel to the naso-occipital axis (positive forward), Y axis parallel to the interaural axis (positive left), and Z axis normal to the X-Y plane (positive upwards). X, Y and Z components mainly reflect the roll, pitch and yaw component, respectively. The rotation vector  $\mathbf{r}$  describing a rotation of  $\theta$  about the axis  $\mathbf{n}$  is given by  $\mathbf{r} = \tan(\theta/2) \cdot \mathbf{n}$ .  $\mathbf{n}$  is a unit vector the direction of which represents the direction of the axis. Because the Euler angle is familiar, using Euler angles given as  $2 \cdot \tan^{-1}$  (magnitude of rotation vector), we represented the eye position as axis-angle representations [10, 11]. The subjects showed some nystagmus when the positioning test was carried out. Using both start and end eye position of slow phase of each nystagmus, we could get rotation vectors as below, which represents the axis of each nystagmus. Setting the start eye position of slow phase of a nystagmus as reference position, end eye position of slow phase of the nystagmus can be represented by the rotation vector of which the reference position is the start eye position of slow phase of the nystagmus, and not the eye position assumes when the subject is looking straight ahead. This rotation vector can change the start eye position of slow phase of the nystagmus to the end position of slow phase of the nystagmus, so the

direction of this rotation vector means the axis of slow phase of the nystagmus. By carrying out the positioning test, we could get the rotation vector whose number was the same as the number of nystagmus. We used the least square method for all these rotation vectors and found the unit vector that passed through the origin. We set this unit vector as the axis of eye rotation and decided the angular velocity by dividing the Euler angle around the axis by the time passed during the slow phase of nystagmus. Finally, we set the time when the velocity reached the peak level to be 0. The velocity changes against time were fit to a single decaying exponential function,  $v = v_0 \exp(-t/T_c)$ , using the least square method.  $v$  represents the velocity of slow phase of nystagmus,  $v_0$  represents the maximum velocity of BPPN,  $t$  represents time, and  $T_c$  represents time constant [12, 13].

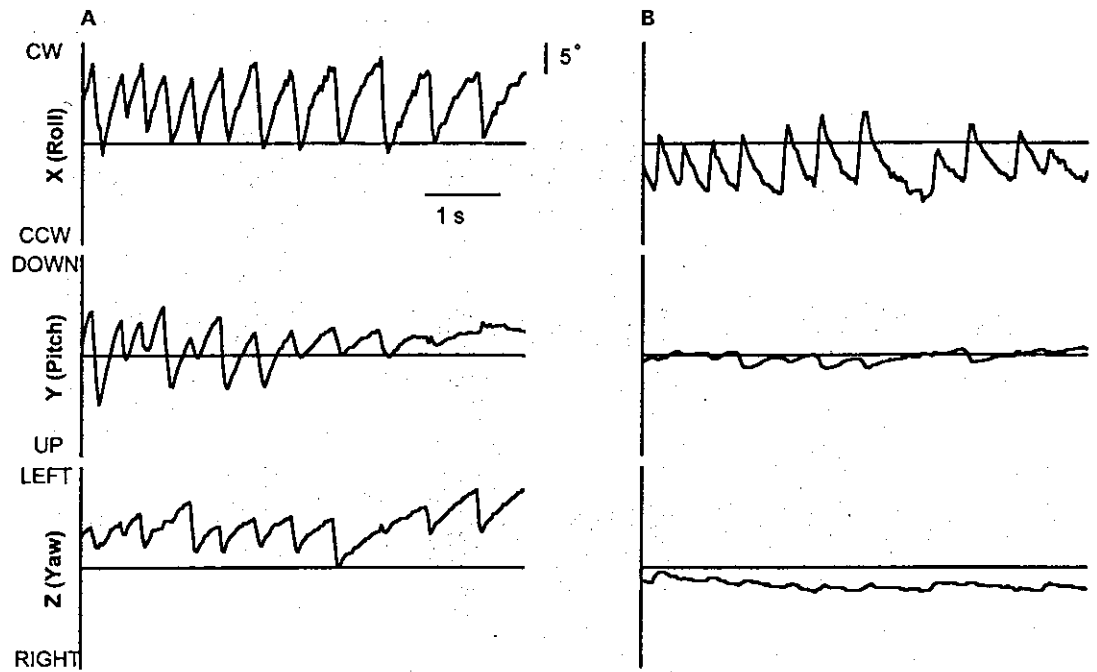
## Results

Figure 1 shows two representative recordings of eye position of BPPN in X (torsion), Y (pitch) and Z (yaw) components. Patient A showed nystagmus that had all components, X, Y, Z (fig. 1A). Patient B showed almost pure torsional nystagmus that had mainly X component, and little Y, Z components (fig. 1B).

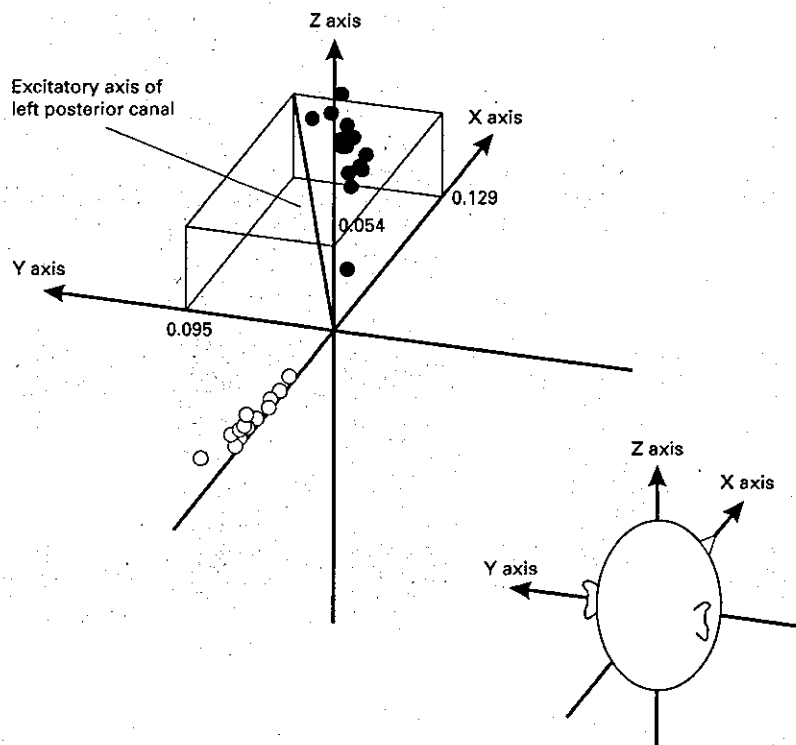
Rotation vectors were calculated from nystagmus of patient A and patient B (fig. 2). The length between the origin and dotted rotation vector means the value of  $\tan$  (the amplitude of nystagmus/2). All rotation vectors that were obtained from each patient were aligned along almost one line. The unit vector of the rotation axis during BPPN was decided using the least square method. All rotation vectors that were obtained from patient A were near the line perpendicular to the left posterior semicircular canal plane [14], while rotation vectors that were obtained from patient B were near the X axis.

Figure 3 shows three-dimensional representations of the rotation axis unit vector of BPPN in 14 patients, as seen from above (fig. 3A), from the right side (fig. 3B) and from the front (fig. 3C). Filled circles indicate unit vectors hypothesized to be induced by excitation of four vertical canals, namely the right anterior and posterior canal and the left anterior and posterior canal [14]. In 8 patients the calculated unit vectors were closely aligned with the excitatory axis of left or right posterior canal, while in the other 6 patients, the unit vectors were closely aligned with X axis.

Figure 4 shows the changes in eye angular velocity around the rotation axis in slow phase of patient A's and patient B's BPPN. The patients' eye angular velocity around the rotation axis in slow phase of BPPN decreased exponentially. Time constants were 4.59 s for BPPN in patient A, and 7.06 s for BPPN in patient B.



**Fig. 1.** Position data that were obtained from patient A (A) and from patient B (B). These data are represented by the Euler angle. A Clear nystagmus could be seen in the X (roll), Y (pitch) and Z (yaw) component. B Clear nystagmus could be seen only in the X component.



**Fig. 2.** Rotation vectors that were obtained from BPPN in patient A laid along the axis perpendicular to the left posterior semicircular canal plane. Rotation vectors that were obtained from BPPN in patient B laid along the X axis. ● = Rotation vectors of BPPN in patient A; ○ = Rotation vectors of BPPN in patient B.

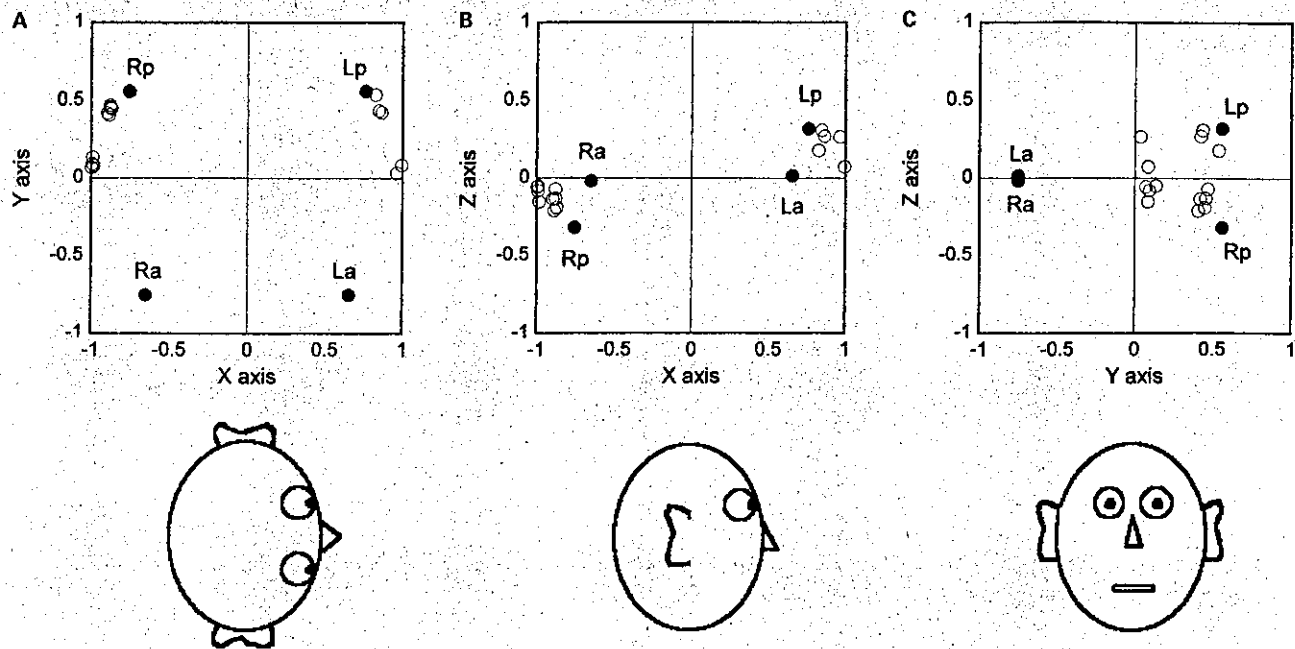


**Fig. 3.** Unit vector of eye rotation axis of BPPN in 14 patients. Unit vector that were perpendicular to the right anterior semicircular canal (Ra); the right posterior semicircular canal (Rp); the left anterior semicircular canal (La), and the left posterior semicircular canal (Lp). Eight unit vectors were near the unit vector perpendicular to the posterior semicircular canal. The other six unit vectors were near the X axis.

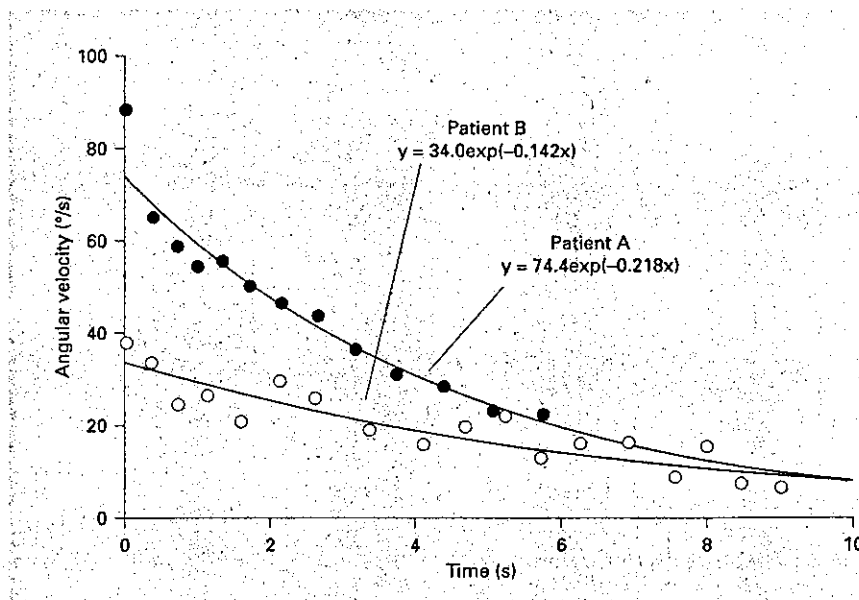


**Fig. 4.** Changes in eye angular velocity around the rotation axis in slow phase of BPPN in patients A and B. These velocities decreased exponentially. Using the least square method, we apply the change of the velocity against time to the following exponential formula:  $y = 74.4\exp(-0.218x)$ , and  $y = 34.0\exp(-0.142x)$ .

**Table 1.** Time constants and maximum angular velocity (patients A–N)

	A	B	C	D	E	F	G	H	I	J	K	L	M	N	Mean (SD)
Time constant, s	4.59	7.04	4.22	2.64	10.31	2.14	7.14	3.33	3.85	7.69	10.00	3.23	13.16	2.97	5.88 (3.41)
Maximum angular velocity, %/s	74.4	34.0	100.9	74.4	55.5	10.7	50.1	10.5	70.3	52.2	28.0	48.4	35.8	47.5	49.5 (25.2)

In table 1, we show time constants and maximum angular velocities that were obtained from all patients. The range of time constant was between 2.14 and 13.16 s, and the mean value was 5.88 s. The range of maximum angular velocity was between 10.5 and 100.9%/s, and the mean value was 49.5%/s.

### Discussion

Two leading theories regarding the pathophysiology of BPPN exist. One is the cupulolithiasis theory [15] and the other is the canalolithiasis theory. The latter theory can best explain the characteristic features of BPPN [3, 4]. According to the canalolithiasis theory, BPPN is caused by a otocania of calcium carbonate crystals which forms at the most dependent portion of the posterior canal when the patient is sitting upright. Movement of the head back and to the side in the plane of posterior canal causes the otocania to move in an ampullofugal direction, producing ampullofugal displacement of the cupula due to the plunger effect of the otocania moving within the narrow canal.

Anatomical studies showed a close coupling between the semicircular canals and the oculomotor system. In addition, electrophysiological study by Suzuki and Cohen [5, 6] demonstrated that electrical stimulation of single semicircular canal afferents in animals induced eye movements that lie in the plane of the canal. In the present study, three-dimensional eye rotation axes of BPPN in 8 patients were closely perpendicular to the posterior canal of the undermost ear in the provocative head position. Under the hypothesis that BPPN is due to a mechanical stimulation of the posterior canal by canalolithiasis, this finding suggested that the posterior canal of the undermost ear is the lesion. Fetter and Sivering [16] have already reported that the eye rotation axis in BPPN is consistent with the axis perpendicular to the posterior semicircular canals.

On the other hand, in the present study, eye rotation axes of torsional BPPN in some patients were closely aligned with the naso-occipital axis. Clinically, it is known that two types of BPPN are observed behind Frenzel

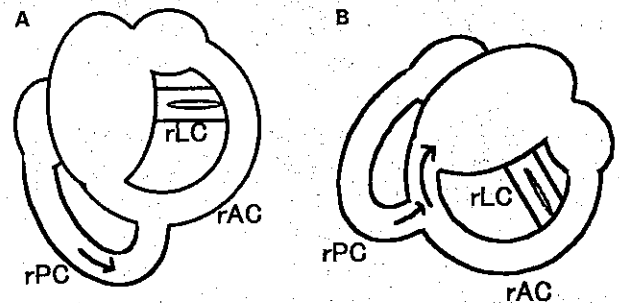


**Fig. 5.** **A** Canalolithiasis induces endolymphatic flow only in the posterior semicircular canal, resulting in vertical and torsional BPPN. **B** Canalolithiasis induces endolymphatic flow in both posterior and anterior canals via the common crus, resulting in torsional BPPN. rLC = Right lateral semicircular canal; rAC = right anterior semicircular canal; rPC = right posterior semicircular canal.

lenses [17]. One type of BPPN has vertical and torsional components. The other type of BPPN has mainly torsional components. The difference in direction in BPPN has been explained by the gaze-dependent effect as followed. Behind Frenzel lenses, BPPN seems to be mainly torsional when gaze is directed towards the undermost ear, but vertical and torsional when gaze is directed towards the uppermost ear [18]. In the present study, however, we analyzed the three-dimensional eye rotation axis in BPPN, which is in head-fixed coordinates, not in eye-fixed coordinates. Rotations about head-fixed axes are often called active rotations or rotations of the objects, since in successive rotations the axes of the successive rotations are unaffected by the preceding rotations of the objects [9]. Indeed, the present findings revealed two types of eye rotation axes of BPPN in head-fixed coordinates. One is BPPN, of which eye rotation axis was closely aligned with the excitatory axis of the posterior canal and beating in vertical and torsional directions. Another one is torsional BPPN, of which eye rotation axis was aligned with the naso-occipital axis. Suzuki and Cohen [5, 6] also showed electrophysiologically that stimulation of two canals produced eye movements that are given by the sum-

mation of the movements induced by stimulation of individual canals. Therefore, the following pathophysiology of torsional BPPN is proposed. Canalolithiasis moves in the posterior canal by the Dix-Hallpike maneuver to induce endolymphatic flow in the posterior and the anterior canals via the common crus. The ampullofugal stimulation in both the anterior and posterior canals then rotates the eye along the naso-occipital axis, resulting in torsional BPPN (fig. 5). The difference between vertical and torsional, and torsional BPPN may depend on the size, weight, viscosity and position of the canalolithiasis or on the speed and trajectory of the head movement by the Dix-Hallpike maneuver. So, it is thought that if the positioning test was induced by the lateral head-trunk tilt [4, 19], the ratio of torsional BPPN became smaller, because the length of the trajectory of the lateral head-trunk tilt is shorter than that of the Dix-Hallpike maneuver. When the length of trajectory is short, the length of otocania movement is short and otocania stops in the posterior canal far from the common crus, so the influence of common crus to BPPN becomes small.

Yagi and Ushio [20, 21] have reported about BPPN analyzed by computerized image recognition method. They analyzed horizontal and vertical eye movement by the movement of center of the pupil. Further, they analyzed rotational eye movement by its particular iris striation in relation to the center of the pupil [22]. Their rotational component means the rotation around the gaze axis and the axis of rotational component changes according to the horizontal and vertical component. They compared the eye movement between BPPN and eye rotation on the vertical semicircular canal plane. However, the horizontal and vertical eye movements are different during BPPN and eye rotation on the vertical semicircular canal plane, making it difficult, using their method, to discuss the relationship between the eye rotation axis of BPPN and the plane of semicircular canals. We believe that using rotation vectors and analyzing eye movements around the head fixed, X, Y and Z axes would be a more appropriate method of establishing the relationship between the eye rotation axis of BPPN and the plane of semicircular canals.

The mean time constant of BPPN was 5.88 s, which was close to post-rotatory nystagmus time constant obtained when the vertical semicircular canal was mainly stimulated [13, 23] and far from the velocity storage time constant obtained when the horizontal semicircular canal was mainly stimulated [12]. This indicates that vertical semicircular canals were mainly stimulated during BPPN. The range and standard deviation of time constant in this

study is smaller than that of velocity storage time constant obtained when the horizontal semicircular canal was mainly stimulated, but larger than that of time constant obtained when the vertical semicircular canal was mainly stimulated. Seidman and Leigh [13] used only torsional component and Morita et al. [23] used only vertical component. But we calculated time constant using the velocity around the axis of rotation. So our data were influenced not only by torsional or vertical component but also by other components. That is considered the reason why the range and standard deviation of our data was large.

It was reported that otolith inputs change the axis of eye rotation toward the gravito-inertial acceleration via velocity storage integrator [24], and that there is a lesion in the otolith system in BPPV patients [25–27], suggesting that there is a possibility that the eye rotation axes are not consistent with the axis perpendicular to the posterior canal or pure torsional axis because of the lesion of otolith system, or that the variation in the axis of eye rotation may indicate an individual anatomical variation of the semicircular canals.

In conclusion, we showed two types of eye movement during BPPN. One is the vertical and torsional eye movement of which the rotation axis lies on the posterior semicircular canal plane, and the origin of which is thought to be the posterior semicircular canal. The other is a pure torsional eye movement thought to originate from the posterior and anterior semicircular canals that are stimulated via the common crus.

### Acknowledgement

We thank Prof. Makoto Igarashi for his critical reading of the manuscript.



ELSEVIER

Auris Nasus Larynx 30 (2003) 233–237

AURIS NASUS  
LARYNX  
INTERNATIONAL JOURNAL  
OF ORI & HNS

www.elsevier.com/locate/anl

## A new rotational test for vertical semicircular canal function

Masahiro Morita<sup>a,\*</sup>, Takao Imai<sup>a</sup>, Sekine Kazunori<sup>b</sup>, Noriaki Takeda<sup>b</sup>,  
Izumi Koizuka<sup>c</sup>, Atsuhiko Uno<sup>a</sup>, Tadashi Kitahara<sup>a</sup>, Takeshi Kubo<sup>a</sup>

<sup>a</sup> Department of Otolaryngology, Minoo Municipal Hospital, Osaka University Medical School, 5-7-1 Kayano Minoo, Osaka 562-8562, Japan

<sup>b</sup> Department of Otolaryngology, Tokushima University Medical School, Tokushima, Japan

<sup>c</sup> Department of Otolaryngology, Saint Marianna Medical School, Kanagawa, Japan

Received 13 August 2002; received in revised form 13 May 2003; accepted 16 May 2003

### Abstract

**Objective:** We developed a new rotating chair in order to assess the function of the vertical semicircular canal (VSCC) by analyzing VSCC-induced post-rotatory nystagmus (PRN). **Methods:** We examined 14 healthy subjects, wearing goggles equipped with an infrared CCD camera, and sitting on a chair which was designed to stimulate a pair of the VSCCs by tilting the head 60° backward with a 45° rotation to the left or right side from the sagittal plane. The time constant (TC) or maximal slow phase eye velocity (MSPEV) of the vertical component of four kinds of PRN were analyzed in four corresponding rotatory conditions, and used as functional index of the corresponding VSCC. **Results:** The mean values of MSPEV in both anterior semicircular canal (ASCC) and posterior semicircular canal (PSCC)-induced PRN tended to be lower ( $P < 0.10$ ) than those induced by the lateral semicircular canal (LSCC). The result suggests that the threshold to the angular velocity in the VSCC is lower than that in the LSCC. The mean values of TC in both ASCC and PSCC-induced PRN were significantly lower ( $P < 0.05$ ) than those induced by the LSCC. **Conclusion:** The significant reduction of TC in VSCC-induced PRN compared with LSCC-induced PRN indicates that VSCC function is less affected by velocity storage mechanisms than LSCC function. The rotational test with respect to the VSCC can be used as a tool for assessing vertical canal function.

© 2003 Elsevier Ireland Ltd. All rights reserved.

**Keywords:** Vertical semicircular canal; Rotational test; Post-rotatory nystagmus; Vestibulo-ocular reflex

### 1. Introduction

Rotational tests have been exclusively used for evaluating the function of the lateral semicircular canal (LSCC). However, there have been only few reports testing vertical semicircular canal (VSCC) function in human [1,2], mainly because of the difficulty to selectively stimulate the VSCC.

The posterior semicircular canal (PSCC) is suspected of being responsible for benign paroxysmal positional nystagmus (BPPN) [2,3]. Moreover, the inferior vestibular nerve, which innervates the PSCC is reported to be the origin of nearly a half of acoustic neuroma [4,5]. Hence the need to examine VSCC function is thought to possess a clinical importance.

In the present study, we first developed a new rotating chair to selectively stimulate a pair of the VSCCs. Tweed et al. reported with three-dimensional axis rotation that post-rotatory nystagmus (PRN) around earth-horizontal axes, but not earth-vertical axes, was influenced by otolith function and other reflexes [6]. Therefore, we used earth-vertical rotation with specific head positions to stimulate VSCCs. An attempt was then made to assess VSCC function by analyzing VSCC-induced PRN [7,8].

### 2. Methods

The subjects were 14 healthy volunteers (nine males, five females) ranging in age from 25 to 36 (mean age 29) years old with no history of any neurologic or otologic disorders. This study was performed in accordance with guidelines approved by the Committee for Medical

\* Corresponding author. Tel.: +81-727-28-2001; fax: +81-727-28-8495.

E-mail address: ent@m.email.ne.jp (M. Morita).



Table 1  
VSCC-induced PRN with respect to the head position under four different conditions

head position tilting 60° backward rotating 45° laterally to	rotation	excitatory canal	nystagmus
right	CW	(r)ASCC	down beating, rotatory(CW)
	CCW	(l)PSCC	up beating, rotatory(CCW)
left	CW	(r)PSCC	up beating, rotatory(CW)
	CCW	(l)ASCC	down beating, rotatory(CCW)*

Ethics of Osaka University Medical School, and an informed consent was obtained from each individual prior to the study.

A new rotating chair (First Co. Ltd., Japan), which was designed to stimulate the VSCC, was developed (Fig. 1). The subject, wearing goggles equipped with an infrared CCD camera, sat on the chair with the head, neck, and back tilted 60° backward (angles values refer

to the earth vertical axis as shown in Fig. 1), and the head was rotated 45° to the left or right side from the sagittal plane. The center of the head was aligned with the rotational axis so that linear acceleration during the rotation affecting the inner ear could be minimized. As shown in Fig. 1, when the head of the subject was tilted 60° and rotated 45° to the left side, the left anterior semicircular canal (ASCC) and the right PSCC were

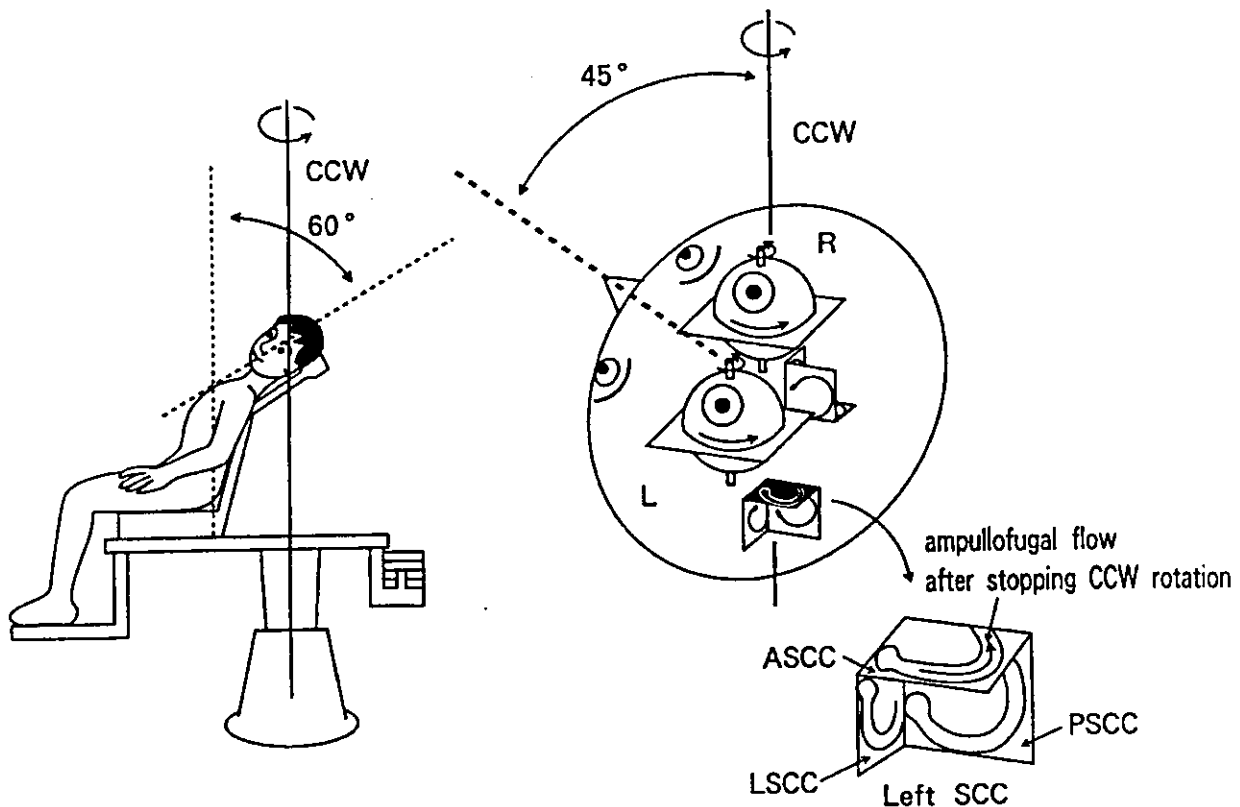


Fig. 1. Schematic illustration of the specific head position, and mechanisms of stimulation of the left ASCC after stopping CCW rotation (Fig. 1, right). Arrows around the eyes indicate the direction of eye movements in a slow phase. CCW, counter-clockwise rotation; PSCC, posterior semicircular canal; ASCC, anterior semicircular canal; LSCC, lateral semicircular canal.

brought together into a plane perpendicular to the rotational axis. The chair was rotated counter-clockwise (CCW) with an initial acceleration of  $2^\circ/s^2$  until the angular velocity reached  $60^\circ/s$ . After per-rotatory nystagmus had subsided, the rotation was then stopped with a deceleration of  $100^\circ/s^2$ . PRN consisted of both down-beating and CCW rotatory (from the subjects point of view) components (\* in Table 1) mainly induced by the excitation of the left ASCC by ampullofugal endolymph flow (Fig. 1) and partly by the inhibition of the right PSCC by ampullopetal endolymph flow. In this condition, we used the down-beating PRN as an index of the left ASCC function. To stay alert with eyes open during rotation in the darkness, subjects were asked to perform mental arithmetic and to look straight ahead during the whole procedure.

The subjects were randomly rotated clockwise (CW) or CCW with right or left head positions. The four kinds of PRN induced by the corresponding four rotatory conditions are shown in Table 1. PRN consisted of both up-beating and CW rotatory components induced by the excitation of the right PSCC after stopping the CW rotation with the head rotating to the left. When the head was rotated  $45^\circ$  to the right, both down-beating and CW rotatory PRN were induced by the excitation of the right ASCC, while both up-beating and CCW rotatory PRN were evoked by the excitation of the left PSCC after stopping the CW or CCW rotation, respectively (Table 1).

Each vertical component of PRN induced by the excitation of a VSCC was recorded and analyzed by an infrared video system with a computer processor (Konan Co. Ltd., Japan). Sampling time of the system was 0.16 ms (60 Hz) and resolution of eye movement analysis was 0.3 and  $0.5^\circ$  in horizontal and vertical axes, respectively. Eyelashes and lid artifacts sometimes hamper to analyze vertical component of eye movement. In order to avoid eyelashes artifact, we curled up the eyelashes, if necessary. In order to avoid lid artifact, during experiment, we instructed subjects to open their eyes widely. Details were described elsewhere [9]. The maximal slow phase eye velocity (MSPEV) of the vertical PRN was measured and its time constant (TC) determined through non-linear regression analysis. Either parameter in response to VSCC stimulation was used as an index of the function of individual canals.

In the conventional rotational testing for LSCC-induced PRN, subjects sat in the upright position with the head tilted forward  $30^\circ$  to the rotational axis. MSPEV and TC in the horizontal PRN were measured and used as an index of LSCC function.

Analysis of variance (ANOVA) with Scheffe's procedure as a post-hoc test and Student's *t*-test were used to determine the significance of difference.

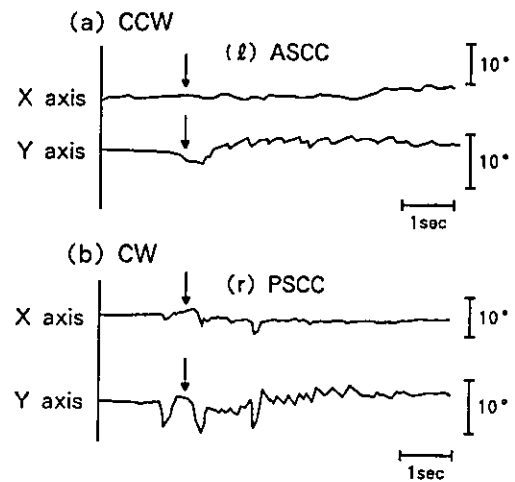


Fig. 2. VSCC-induced PRN. (a) The down beating nystagmus induced by left ASCC stimulation in the condition shown. CCW, counter-clockwise rotation. (b) The up beating nystagmus induced by right PSCC stimulation at the termination of CW with the specific head position shown in Fig. 1. The longitudinal bars represent degrees of eye position.

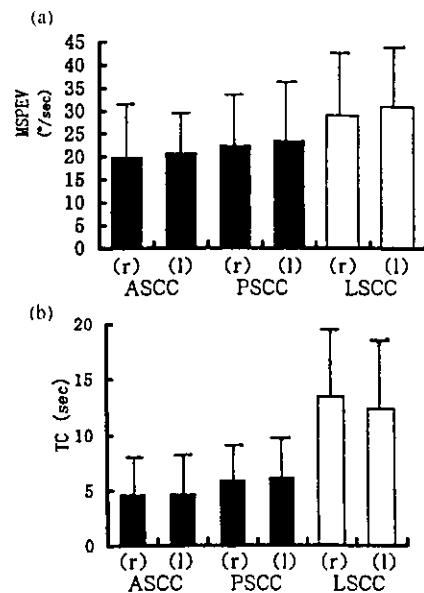


Fig. 3. (a) MSPEV of the vertical component of PRN induced by the VSCC and horizontal component of PRN induced by the LSCC. The columns and bars indicate the mean  $\pm$  S.D. of MSPEV. (b) TC of the vertical component of PRN induced by the VSCC and horizontal component of PRN induced by the LSCC. The columns and bars indicate the mean  $\pm$  S.D. of TC.

### 3. Results

Fig. 2 shows vertical and horizontal eye movements of the PRN induced by the excitation of the left ASCC (Fig. 2a) and the right PSCC (Fig. 2b), in the specific head position, as shown in Fig. 1. MSPEV and TC of the vertical or horizontal components of PRN induced

by excitatory stimulation of individual vertical or horizontal semicircular canals are shown in Fig. 3. The mean values of MSPEV (Fig. 3a) in both ASCC and PSCC-induced PRN tended to be lower, compared with those induced by the LSCC (ANOVA:  $F(5, 78) = 2.08$ ,  $P = 0.076$ ). The mean values of TC (Fig. 3b) in both ASCC and PSCC-induced PRN were significantly lower than those induced by the LSCC (ANOVA:  $F(5, 78) = 12.18$ ,  $P < 0.001$ ; Scheffe's procedure as a post-hoc test,  $P < 0.05$ ). However, there were no significant differences in MSPEV or TC between ASCC and PSCC-induced PRN. The differences between the left and right side in MSPEV and TC in ASCC, PSCC and LSCC-induced PRN were not significant (paired Student's *t*-test).

#### 4. Discussion

In order to evaluate VSCC function, we developed a rotational test using a newly designed rotating chair where the patient sat in a specific head position. The semicircular canals lie approximately at right angles to each other [10]. A recent study with computer-aided three dimensional reconstructions of human temporal bone reported that the angles from sagittal plane are  $41^\circ$  to the ASCC and  $56^\circ$  to the PSCC [11]. The PSCC is approximately parallel to the ASCC in the opposite side. Therefore, tilting the head  $60^\circ$  backward with a  $45^\circ$  lateral rotation brings the pair of VSCCs (ASCC and PSCC) into a plane perpendicular to the rotation axis (Fig. 1). In accordance with the Ewald's law, the VSCC are activated by ampullofugal endolymph flow and inhibited by ampullopetal flow [12]. Accordingly, with the specific head position, it is likely that PRN was induced by both the excitation of one VSCC and the inhibition of the other.

PRN induced by a pair of the VSCCs consisted of both vertical and rolling eye movements, which are in line with the works of Suzuki [13], and Cohen [14] who reported eye movements evoked by singular nerve stimulation of individual semicircular canals. Our data support these findings. For example, in the rotational condition shown in Fig. 1, downward beating PRN mixed with CCW rotatory component (Fig. 2a), mainly due to the excitation of left ASCC were induced after stopping the CCW rotation (\* in Table 1). Each vertical and rotatory component of PRN with respect to the head position and rotational direction are summarized in Table 1. We used the vertical components of VSCC-induced PRN as an index of the function of the corresponding VSCC, on the basis of excitatory stimulation for individual VSCCs.

The mean values of MSPEV in VSCC-induced PRN tended to be smaller than those of the LSCC (Fig. 3a). The differences in the mean values of MSPEV between

VSCC and LSCC-induced PRN should be due to the differences in the sensitive threshold level to the angular velocity. Decher et al. demonstrated by using VSCC stimulative rotation that the threshold in the VSCC was, on average, twice as high as that of the LSCC [1]. LSCC-induced PRN contains only horizontal component while VSCC-induced PRN consists of both vertical and rolling components. Therefore, the reduction of those values in VSCC-induced PRN might be also caused by the measurement of only vertical component for VSCC function in this study. To overcome the problem, a vector analysis of eye movement is useful. Recently, we developed a new technique for analyzing the rotation vector of eye movement with infrared CCD camera [15]. MSPEV around the axis of eye rotation, in other words, eye velocity vector of VSCC-induced PRN can be more accurate index of VSCC function.

The significantly larger differences in TC between LSCC- and VSCC-induced PRN were reported in the present study despite the insignificant differences in MSPEV. TC value of horizontal component in LSCC-induced PRN was approximately the same as those which were reported by other authors [16]. The TC in the VOR is determined by the so-called velocity storage mechanisms [17], which have been shown to prolong the TC of the VOR above the value predicted from peripheral mechanics alone [18]. The obviously shortened TC in VSCC-induced PRN (Fig. 3b) indicates that VSCC-induced PRN is less affected by velocity storage mechanisms as compared with LSCC-induced PRN.

The rotational test has been usually performed in the examination for LSCC function. In the preliminary clinical study, we used our rotational test and found that MSPEV of PSCC-induced PRN was suppressed in the affected side of a patient with cholesteatoma destroying the PSCC. Moreover, we also found that MSPEV of PSCC-induced post- and per-rotatory nystagmus was suppressed in the affected side of patients with acoustic neurinoma. These results in the preliminary study propose that VSCC-induced PRN can be used for the diagnosis of the balance disorders.

In conclusion, the rotational test with respect to the VSCC can be used as a tool for assessing vertical canal function.

#### References

- [1] Decher H. Experimental labyrinthine tests on isolated individual semicircular canals as a fitness test for astronauts. *Aerospace Med* 1969;40:1203–8.
- [2] Fetter M, Sievering F. Three-dimensional eye movement analysis in benign paroxysmal positional vertigo and nystagmus. *Acta Otolaryngol (Stockholm)* 1995;115:353–7.
- [3] Hall SF, Ruby RRF, McClure JA. The mechanics of benign paroxysmal vertigo. *J Otolaryngol* 1979;8:151–8.

- [4] Ylikoski J, Palva T, Collan Y. Eighth nerve in acoustic neuromas: special reference to superior vestibular nerve function and histopathology. *Arch Otolaryngol* 1978;104:532–7.
- [5] Hashimoto S, Kawase T, Furukawa K, Takasaka T. Strategy for the diagnosis of small acoustic neuroma. *Acta Otolaryngol (Stockholm)* 1991(suppl 481):567–9.
- [6] Tweed D, Fetter M, Sievering D, Misslisch H, Koenig E. Rotational kinematics of the human vestibuloocular reflex. II. Velocity steps. *J Neurophysiol* 1994;72:2480–9.
- [7] Morita M. Testing of vertical semicircular canal-stimulative postrotatory nystagmus: preliminary study in normal subjects. *Equilib Res* 1993;52:461–5.
- [8] Morita M, Takeda N, Koizuka I, Kubo T. Vertical semicircular canal-stimulative post-rotatory nystagmus: comparison of the nystagmus induced by lateral semicircular canal-stimulation in normal adult subjects. *Equilib Res* 1996;55:380–6.
- [9] Kubo T, Saika T, Sakata Y, Morita M. Analysis of saccadic eye movements using an infrared video system in human subjects. *Acta Otolaryngol (Stockholm)* 1991(suppl 481):382–7.
- [10] Curthoys IS, Blanks RHJ, Markham CH. Semi-circular canal functional anatomy in cat, guinea pig and man. *Acta Otolaryngol (Stockholm)* 1977;83:258–65.
- [11] Takagi A, Sando I, Takahashi H. Computer-aided three-dimensional reconstruction of semicircular canals and their cristae in man. *Acta Otolaryngol (Stockholm)* 1989;107:362–5.
- [12] Baloh RW, Honrubia V, Konrad HR. Ewald's second law reevaluated. *Acta Otolaryngol (Stockholm)* 1977;83:475–9.
- [13] Suzuki JI, Goto K, Tokumasu K, Cohen B. Implantation of electrodes near individual vestibular nerve branches in mammals. *Ann Otol Rhinol Laryngol* 1969;78:815–26.
- [14] Cohen B, Suzuki JI. Eye movements induced by ampullary nerve stimulation. *Am J Physiol* 1963;204:347–51.
- [15] Imai T, Takeda N, Morita M, Koizuka I, Kubo T, Miura K, Nakamae K, Fujioka H. Rotation vector analysis of eye movement in three dimensions with an infrared CCD camera. *Acta Otolaryngol* 1999;119:24–8.
- [16] Fetter M, Hain TC, Zee DS. Influence of eye and head position on the vestibulo-ocular reflex. *Exp Brain Res* 1986;64:208–16.
- [17] Raphan T, Matsuo V, Cohen B. Velocity storage in the vestibulo-ocular reflex arc (VOR). *Exp Brain Res* 1979;35:229–48.
- [18] Magnusson M, Brantberg K, Pyykkö I, Schalén L. Reduction of the time constant in the VOR as a protective mechanism in acute vestibular lesions. *Acta Otolaryngol (Stockholm)* 1989(Suppl. 468):329–32.